Carbohydrate Polymers 75 (2009) 95–103

Contents lists available at ScienceDirect

Carbohydrate Polymers

journal homepage: www.elsevier.com/locate/carbpol

Low molecular weight chitosan-*g*-L-phenylalanine: Preparation, characterization, and complex formation with DNA

Rangrong Yoksan [a], Mitsuru Akashi [b,*]

[a] Department of Packaging Technology and Materials, Faculty of Agro-Industry, Kasetsart University, Bangkok 10900, Thailand
[b] Department of Applied Chemistry, Graduate School of Engineering, Osaka University, Osaka 565-0871, Japan

ARTICLE INFO

Article history:
Received 13 November 2007
Received in revised form 26 June 2008
Accepted 1 July 2008
Available online 8 July 2008

Keywords:
Chitosan
Phenylalanine
DNA
Nanoparticle
Complex coacervation
DNA release

ABSTRACT

The grafting of L-phenylalanine onto low molecular weight chitosan is accomplished by using carbodiimide as a coupling agent. As increase in the amount of phenylalanine in feed, the grafting chain length increases, while a number of grafting chains hardly change. The obtained product, LMWCts-*g*-Phe, performs sphere with an average size of ~80 nm when the % grafting is less than 123. The complexes of the LMWCts-*g*-Phe and DNA (LMWCts-*g*-Phe/DNA) prepared by a complex coacervation method possess various shapes with an average size of ~50–150 nm and a negatively charged surface. The LMWCts-*g*-Phe and its complex show very reduced toxicity to fibroblast cells. The release of DNA from the complex is very fast in high pH media (tris buffer, pH 8.0 and carbonate buffer, pH 9.5), and relatively slow or more sustainable in neutral and low pH ones (PBS, pH 7.4 and citric acid/trisodium citrate buffer, pH 3.0). The results suggest that the LMWCts-*g*-Phe be an alternative promising carrier for negatively charged active molecules.

1. Introduction

Glycosaminoglycans (GAGs) or mucopolysaccharides are long unbranched polysaccharides consisting of repeating disaccharide units containing amino sugars, at least one of which has a negatively charged side group, i.e., carboxylate or sulphate. In nature, GAGs are covalently attached to a core protein to form proteoglycans, which are the major components of the animal extracellular matrix.

Chitin-chitosan is a plentiful mucopolysaccharide and serves as a structural polysaccharide for many phyla of lower plants and animals. Although chitosan is a linear cationic polymer, it consists of glucosamine and *N*-acetylglucosamine frequently found in a number of GAGs. For many decades, chitosan has been widely accepted as a material for tissue engineering and a carrier for various bioactive compounds owing to its biodegradable, biocompatible, and bioactive properties (Ravi Kumar, Muzzarelli, Muzzarelli, Sashiwa, & Domb, 2004). Recently, the conjugation of natural substances, particularly peptides, to chitosan through one or both amino hydrogen(s) is of interest because it not only provides a unique combination of functional properties, but also improves the solubility of chitosan.

Chitosan-peptide derivatives have received much attention in many areas (Beena, Thomas, & Sharma, 1994; Ishii, Minegishi, Lavitpichayawong, & Mitani, 1995) including drug delivery and tissue engineering (Zhu et al., 2002; Batista, Pinto, Gomes, & Gomes, 2006; Gomes, Gomes, Batista, Pinto, & Silva, 2008). Numerous efforts have been made to prepare such derivatives. For instance, amino acids were covalently attached to chitosan by the coupling reaction using carbodiimide and/or glutaraldehyde (Beena et al., 1994; Kurita, Hayakawa, Nishiyama, & Harata, 2002; Zhu et al., 2002) and the reductive amination of aldehydes and ketones (Muzzarelli, Tanfani, Emanuelli, & Bolognini, 1985). In some cases, either chitosan or peptide was firstly modified and then reacted with the other. Ishii et al. (1995) have reported the preparation of chitosan-amino acid conjugates via the reaction of glyoxylic acid-substituted chitosan and amino acid. On the other hands, the water soluble *N*-(γ-propanoyl-amino acid)-chitosans have been synthesized using peptide ligands, which were obtained from the condensation between bromopropanoic acid and natural α-amino acids, and chitosan as starting materials (Batista et al., 2006; Gomes et al., 2008). In addition, many studies have attempted to improve the cell adhesion of chitosan scaffolds and membranes by immobilizing the specific peptide sequences or RGD-containing peptide(s) using carbodiimide and hydroxysuccinamide to form imide bond (Ho et al., 2005), glutaraldehyde to form Schiff base (Kirsebom et al., 2007), and photochemical technique (Chung, Lu, Wang, Lin, & Chu, 2002; Chung et al., 2003; Karakecili & Gumusderelioglu, 2008). Although Chi, Wang, and Liu (2008) have developed a water soluble chitosan-graft-poly (L-lysine) via the heterogeneous ring opening polymerization of N_{ε}-carbobenzyloxy-L-lysine NCA in

* Corresponding author. Tel.: +81 6 6879 7357; fax: +81 6 6879 7359 (M. Akashi).
E-mail address: akashi@chem.eng.osaka-u.ac.jp (M. Akashi).

0144-8617/$ - see front matter © 2008 Elsevier Ltd. All rights reserved.
doi:10.1016/j.carbpol.2008.07.001

water/ethyl acetate, few publications about chitosan-polypeptide derivatives were revealed.

DNA, a negatively charged macromolecule, has been reported to form complexes with cationic polymers (Segura, Volk, & Shea, 2003; Ravi Kumar, Bakowsky, & Lehr, 2004; Li et al., 2006) including chitosan, providing polymeric vectors used in nonviral delivery systems (Lee et al., 2001; Mao et al., 2001; Koping-Hoggard, Mel'nicova, Varum, Lindman, & Artursson, 2003, 2004; Bozkir & Saka, 2004; Kiang, Wen, Lim, & Leong, 2004; Son et al., 2004; Lee, 2005; Peng et al., 2005; Hu et al., 2006). Recently, chitosan/DNA (Mao et al., 2001; Bozkir & Saka, 2004; Kiang et al., 2004), LMWCts/DNA and/or chitosan oligomer/DNA (Richardson, Kolbe, & Duncan, 1999; Lee et al., 2001; Koping-Hoggard et al., 2003, 2004; Peng et al., 2005), as well as their derivatives/DNA complexes (Son et al., 2004; Lee, 2005; Hu et al., 2006) have been proposed for overcoming problems with toxicity and low transfection efficiency of other cationic polymers such as poly-L-lysine (Choi et al., 1998) and polyethylenimine (Godbey, Wu, & Mikos, 2001; Kean, Roth, & Thanou, 2005). However, the use of chitosan-peptide derivative as a condensing agent and/or carrier for DNA has not been reported.

The present work focuses on two points of view; (i) the preparation of low molecular weight chitosan (LMWCts) grafting with L-phenylalanine (LMWCts-*g*-Phe) using carbodiimide as a coupling agent under mild condition, and (ii) the complex formation of LMWCts-*g*-Phe and DNA (LMWCts-*g*-Phe/DNA). For the latter point of view, we investigate not only the morphology and surface charge of the complex, but also the *in vitro* cytotoxicity and DNA release to propose a feasibility of LMWCts-*g*-Phe as a carrier for negatively charged bioactive molecules. Here, LMWCts is comparatively discussed.

2. Experimental section

2.1. Materials

Chitosan (degree of deacetylation (DD) = 0.8) was purchased from TCI, Japan. L(-)-phenylalanine (Phe), hydrogen peroxide, ethanol, sodium hydroxide, acetone, citric acid, tris(hydroxymethyl)aminomethane, 0.1 M hydrochloric acid, sodium carbonate, sodium bicarbonate, sodium hydrogen phosphate, potassium chloride, potassium phosphate, monobasic (KH_2PO_4), sodium chloride, and trypsin were obtained from Wako Pure Chemical Industries, Ltd., Japan. 1-Hydroxy-1H-benzotriazole, monohydrate (HOBt), 1-ethyl-3-(3-dimethylaminopropyl)-carbodiimide, hydrochloride (EDC), and 2-(4-iodophenyl)-3-(4-nitrophenyl)-5-(2,4-disulfophenyl)-2H-tetrazolium, monosodium salt (WST-1) were supplied by Dojindo, Japan. Trisodium citrate and sodium sulfate were purchased from Chameleon Reagent, Japan. Deuterium oxide (D_2O) and acetic acid-d4 (CD_3COOD) were obtained from Cambridge Isotope Laboratories, Inc., USA. DNA-Na-HP (Lot No. PS-1057) from fish was supplied by Yuki Gosei Kogyo Co., Ltd., Japan. Dulbecco's modified eagle medium (DMEM) was purchased from Invitrogen/Gibco, UK. Fetal bovine serum (FBS) was obtained from Trace Scientific Ltd., Australia. All chemicals were used as received and without further purification.

2.2. Instruments and equipment

The chemical structure was characterized by FT-IR, ^{1}H NMR, and elemental analysis (EA) techniques. FT-IR spectra were recorded on a PerkinElmer Spectrum 100 FT-IR spectrometer in the attenuated total reflection (ATR) mode with 16 scans at a resolution of 4 cm^{-1} over a wavenumber range of 4000-400 cm^{-1}. ^{1}H NMR patterns were obtained at 400 MHz with a JEOL GSX 400 at 70 ± 1 °C for chitosan starting material and 25 ± 1 °C for LMWCts and LMWCts-*g*-Phe. EA was carried out using a Yanako CHN CORDER MT-3, MT-5 analyzer with a combustion temperature at 950 °C under air with O_2 as a combustion gas (flow rate of 20 mL/min) and He as a carrier (flow rate of 200 mL/min). The weight average molecular weight (M_w) was determined by a TOSOH GPC-8020 using pullulan (Shodex standard P-82 kit) as a standard and phosphate buffer (pH 7.4) as a mobile phase (flow rate of 1 mL/min). The packing structure was characterized by X-ray diffraction (XRD). XRD patterns were recorded over a 2θ range of 5–50° by a Rigaku X-ray diffractometer (Model: UltraX 18HB450) operating at a 40 kV and 200 mA. The morphology was observed by SEM and TEM techniques. Sample suspension (5-10 μL) was dropped on a glass slide placed on a SEM stage using double-sided carbon adhesive tape, and then dried under reduced pressure overnight. Dried samples were coated with OsO_4 of 5 nm thick by a HPC-30 plasma coater (Vacuum Device Inc.) before observation by a JEOL JSM-6700FE field emission scanning electron microscope at a 15 kV. For TEM, sample suspension (5–10 μL) was dropped on a copper grid, dried under reduced pressure overnight, and deposited with carbon of 5–10 nm thick by a JEOL JEE-420 vacuum evaporator. TEM images were visualized with a JEOL JEM-100CX II electron microscope at an 80 kV operation. The zeta potential was determined at 20 °C by a Malvern Zetasizer Nano Series equipped with a He–Ne laser operating at 4.0 mW and 633 nm with a fixed scattering angle of 90°. The amount of DNA in supernatant was measured by a Hitachi U-3010 spectrophotometer with a scan speed of 60 nm/min over a wavelength range of 200–400 nm (λ_{max} = 258 nm).

2.3. Preparation of low molecular weight chitosan (LMWCts)

LMWCts was prepared by oxidative degradation as reported elsewhere (Tsuguhei & Tatsuaki, 1997; Wu et al., 2005). Briefly, chitosan (1 g, 5.90×10^{-3} mol equiv. to pyranose ring) was dispersed in distilled water (30 mL) at ambient temperature for 1 h. The dispersion was heated to 60 °C and 30% aqueous H_2O_2 (1 mL, 9.79×10^{-3} mol) was, then, gradually added. The mixture was stirred at 60 °C for 6 h and neutralized with 1 M NaOH followed by filtration to remove high molecular weight polymer. The supernatant was concentrated in a rotary evaporator and was reprecipitated in ethanol. The precipitate was washed repeatedly in ethanol and dried under reduced pressure overnight to give a fine yellowish powder.

Chitosan: FT-IR (cm^{-1}): 3287 (OH), 2882 (C–H stretching), 1651 (C–O, amide I), 1550 (NH, amide II), 1026 (C–O–C), and 896 (pyranose ring). ^{1}H NMR (1% CD_3COOD in D_2O, 70 ± 1 °C, δ, ppm): 2.43 (3H, C<u>H</u>$_3$), 3.57 (1H, H-2), 4.07 (2H, H-5,6), 4.27 (3H, H-3,4,6), and 5.24 (1H, H-1).

LMWCts: FT-IR (cm^{-1}): 3266 (OH), 2860 (C–H stretching), 1617 (C–O, amide I), 1573 (NH, amide II), 1029 (C–O–C), and 879 (pyranose ring). ^{1}H NMR (D_2O, 25 ± 1 °C, δ, ppm): 2.08 (3H, C<u>H</u>$_3$), 3.03 (1H, H-2), 3.79 (2H, H-5,6), 3.95 (3H, H-3,4,6), and 4.59 (1H, H-1). GPC: M_w = 4405 and M_w/M_n = 1.674.

2.4. Preparation of LMWCts-*g*-L-phenylalanine (LMWCts-*g*-Phe)

The preparation of LMWCts-*g*-Phe is summarized in Scheme 1. LMWCts (DD = 0.76, 0.1 g, 2.27×10^{-5} mol) was dissolved in distilled water (5 mL) at room temperature. To a homogeneous solution, Phe, HOBt (1.5 mol equiv. to Phe), and EDC (1.5 mol equiv. to Phe) were added, respectively. The quantity of Phe were varied for 0.5, 1.0, 2.0, 3.0, and 5.0 mol equiv. to pyranose ring or 0.29×10^{-3}, 0.58×10^{-3}, 1.17×10^{-3}, 1.75×10^{-3}, and 2.92×10^{-3} mol, respectively. The mixture was stirred at 4 °C for 30 min and then room temperature overnight. Acetone was used to precipitate the

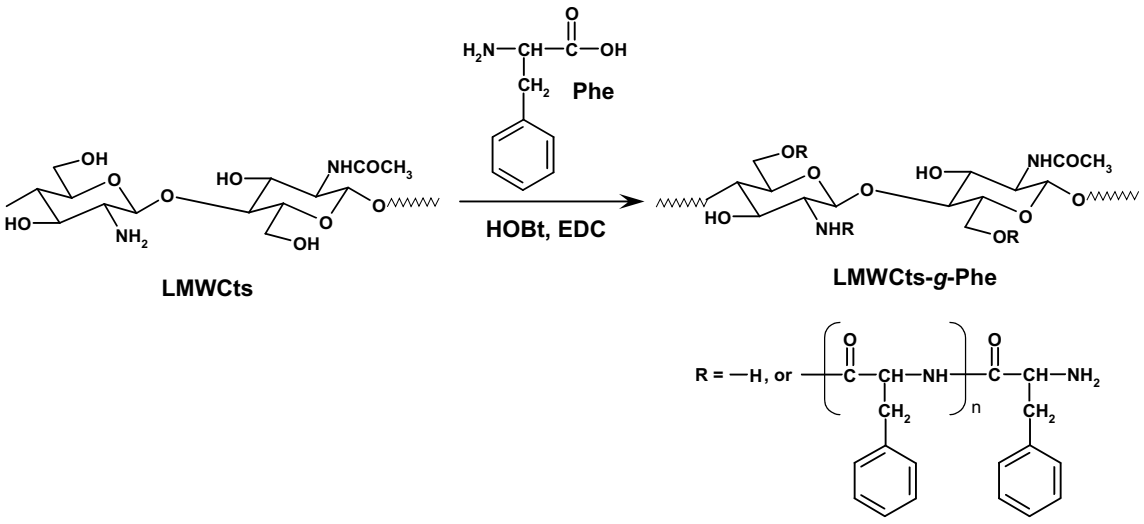

Scheme 1. Preparation of LMWCts-*g*-Phe.

product from the transparent solution. The precipitate was repeatedly washed with acetone and dried under reduced pressure overnight to provide a yellowish or white powder of LMWCts-*g*-Phe0.5, LMWCts-*g*-Phe1, LMWCts-*g*-Phe2A, LMWCts-*g*-Phe3, and LMWCts-*g*-Phe5 according to the quantity of Phe in feed. The LMWCts-*g*-Phe2B was prepared by the same method as LMWCts-*g*-Phe2A, but the amount of HOBt and EDC was 3.0 mol equiv. to Phe.

LMWCts-*g*-Phe: FT-IR (cm^{-1}): 3288, 3088 (OH, NH), 2936, 2884 (C–H stretching), 1730 (COO, ester), 1640 (C–O, amide I), 1557 (NH, amide II), 1033 (C–O–C), 948 (pyranose ring), and 700, 525 (aromatic). ^{1}H NMR (D_2O, 25 ± 1 °C, δ, ppm): 2.08 (3H, C$\underline{H}_3$ of acetamide), 2.90 (1H, H-2), 3.13–3.35 (2H, C$\underline{H}_2$ of Phe), 3.70 (2H, H-5,6), 3.79 (3H, H-3,4,6), 4.00–4.03 (1H, C$\underline{H}$ of Phe), 4.58 (1H, H-1), and 7.34–7.47 (5H, $C_6\underline{H}_5$).

LMWCts-*g*-Phe0.5: Anal. Calcd for $(C_6H_{11}O_4N)_{0.73}(C_8H_{13}O_5N)_{0.23}(C_{123}H_{128}O_{17}N_{14})_{0.04}$ (%): C, 52.89; H, 6.42; and N, 8.44. Found (%): C, 44.77; H, 6.25; and N, 7.28. LMWCts-*g*-Phe1: Anal. Calcd for $(C_6H_{11}O_4N)_{0.73}(C_8H_{13}O_5N)_{0.23}(C_{240}H_{245}O_{30}N_{27})_{0.04}$ (%): C, 56.03; H, 6.18; and N, 8.46. Found (%): C, 48.70; H, 6.17; and N, 7.66. LMWCts-*g*-Phe2A: Anal. Calcd for $(C_6H_{11}O_4N)_{0.73}(C_8H_{13}O_5N)_{0.23}(C_{474}H_{479}O_{56}N_{53})_{0.04}$ (%): C, 58.84; H, 5.91; and N, 8.42. Found (%): C, 50.19; H, 6.14; and N, 7.71. LMWCts-*g*-Phe2B: Anal. Calcd for $(C_6H_{11}O_4N)_{0.73}(C_8H_{13}O_5N)_{0.23}(C_{474}H_{479}O_{56}N_{53})_{0.04}$ (%): C, 56.40; H, 5.66; and N, 8.07. Found (%): C, 49.61; H, 6.27; and N, 7.95. LMWCts-*g*-Phe3: Anal. Calcd for $(C_6H_{11}O_4N)_{0.73}(C_8H_{13}O_5N)_{0.23}(C_{708}H_{713}O_{82}N_{79})_{0.04}$ (%): C, 57.88; H, 5.54; and N, 8.07. Found (%): C, 52.10; H, 6.23; and N, 8.24. LMWCts-*g*-Phe5: Anal. Calcd for $(C_6H_{11}O_4N)_{0.73}(C_8H_{13}O_5N)_{0.23}(C_{1176}H_{1181}O_{134}N_{131})_{0.04}$ (%): C, 58.83; H, 5.38; and N, 8.00. Found (%): C, 54.23; H, 6.44; and N, 8.55.

2.5. Complex formation of LMWCts-g-Phe and DNA

The preparation of complex of LMWCts-*g*-Phe and DNA (LMWCts-*g*-Phe/DNA) was carried out by a complex coacervation method. Two solutions of sample and DNA were separately prepared. Sample (LMWCts-*g*-Phe0.5 and LMWCts-*g*-Phe1) was dissolved in water to get the final concentrations of 1, 2, 3, 4, and 5 mg/mL, while DNA was dissolved in a 50 mM aqueous sodium sulfate solution to obtain 0.01, 0.05, and 0.1 mg/mL. Both solutions were preheated at 50 °C. Sample solution (250 μL) was, then, gradually dropped into the DNA solution (250 μL) during vortex at the highest speed for 30 s. The mixture was placed at ambient temperature for 30 min to assure that the complex was completely formed. The complex solution was divided into two parts; one for zeta potential measurement and the other for SEM and TEM observations. For electron microscopy, the complex was collected by centrifugation and thoroughly washed with water to remove free DNA, free sample, and sodium sulfate salt and, then, resuspended in water before sample preparation in the next step (see Section 2.2).

All complexes used in the studies of cytotoxicity (see Section 2.7) and DNA release (see Section 2.8) were prepared from 1 mg/mL of sample solution and 0.1 mg/mL of DNA solution. The obtained complexes were repeatedly washed with water, rinsed with ethanol, and dried under reduced pressure overnight.

The complex of LMWCts and DNA (LMWCts/DNA) was also prepared by the same method and used as a comparative material.

2.6. Determination of DNA loading efficiency

The solution of sample in water (1, 2, 3, 4, and 5 mg/mL) was gradually dropped into the solution of DNA in 50 mM aqueous Na_2SO_4 (0.1 mg/mL) at 50 °C during vortex at the highest speed for 30 s. After complex was completely formed at ambient temperature for 30 min, the turbid solution was centrifuged and the supernatant was collected to determine the amount of free DNA. The % DNA loading efficiency was calculated by the following equation:

% DNA loading efficiency = $[(A - B)/A] \times 100$; when A = total concentration of DNA (mg/mL) and B = concentration of unloaded DNA (mg/mL).

2.7. In vitro cytotoxicity test

Mouse connective tissue fibroblasts, L929, were applied as model cells for the *in vitro* cytotoxicity study. The fibroblasts (5×10^4 cells per well) were seeded into a 24-well plate (Iwaki, Japan) containing DMEM culture medium with 10% FBS. The seeded plate was, then, incubated for 2 h at 37 °C in a HIRASAWA CPD-170 CO_2 incubator with a humidified 5% CO_2/95% air atmosphere to allow the cells adhere to the well. Samples were dissolved (in the cases of LMWCts and LMWCts-*g*-Phe) or dispersed (in the cases of complexes, i.e., LMWCts/DNA and LMWCts-*g*-Phe/DNA) in DMEM culture medium (1 mg/mL) and fed into each well contain-

ing pre-incubated cells to get the final sample concentrations of 0.1, 0.2, 0.3, 0.4, and 0.5 mg/mL and final volume of 2 mL. After incubation for an additional 22 h at 37 °C in a humidified 5% CO_2/95% air atmosphere, the morphology of cells was observed using a Nikon DIAPHOT TMD-1S optical microscope equipped with a Nikon COOLPIX 950 digital camera, and the number of viable cells was determined by WST-1 method (Berridge, Tan, McCoy, & Wang, 1996). All samples and media were removed leaving adhering cells (living cells) and each well was washed with PBS (1 mL). Then, DMEM medium without the addition of phenol red (490 μL) and WST-1 (10 μL) were added to each well following by incubation for 2 h at 37 °C in a humidified 5% CO_2/95% air atmosphere. The absorbance at 450 nm was recorded using a BIO-RAD 680 96-well microplate reader that was blanked with DMEM medium without the addition of phenol red.

DMEM medium without sample was also prepared by the same protocol and used as a control (100% viability). The % viability was calculated by the following equation:

% Viability = [A/B] × 100; where A = the number of cells in a sample well and B = the number of cells in a control well.

2.8. Study on in vitro DNA release

A series of buffers, i.e., citric acid/trisodium citrate (pH 3.0), phosphate buffer saline (PBS, pH 7.4), tris buffer (pH 8.0), and carbonate buffer (pH 9.5) was used as media for the DNA release study. Dried complex (3.9 mg) and buffer solution (1.2 mL) were placed in a micro tube (SARSTEDT, Germany) and incubated in a water bath (THEMO MAX TM-1, AS ONE, Japan) at 37 ± 0.5 °C. At the sampling time, the incubated dispersing solution was centrifuged, and 400 μL of supernatant was collected for evaluation of the amount of released DNA using a spectrophotometer at 258 nm. An equal volume of fresh buffer was, then, replaced in the solution and the same procedure was repeated for the next sampling time.

3. Results and discussion

3.1. Preparation and characterization of LMWCts

The product obtained from treating chitosan with aqueous H_2O_2 at 60 °C for 6 h was investigated to clarify whether the primary structure (D-glucosamine and *N*-acetyl-D-glucosamine units) of chitosan was retained by using FT-IR and ^{1}H NMR techniques. The product showed the characteristic peaks at 3266 (OH), 2860 (C–H stretching), 1617 (C–O, amide I), 1573 (NH, amide II), 1029 (C–O–C), and 879 cm^{-1} (pyranose ring) (Fig. 1b) as well as the proton peaks at 2.08 ($C\underline{H}_3$ acetamide), 3.03 (H-2), 3.79 (H-5,6), 3.95 (H-3,4,6), and 4.59 ppm (H-1) (Fig. 2b). The results confirmed that the primary structure of the product was similar to that of chitosan (Figs. 1 and 2a). The M_w of the product was ~4405 Dalton as determined by GPC and the degree of deacetylation was ~0.76 by ^{1}H NMR corresponding to ~26 pyranose units (20 U of D-glucosamine and 6 U of *N*-acetyl-D-glucosamine). It was, thus, concluded that the oxidative degradation of chitosan by H_2O_2 provided LMWCts with retained primary structure. For the packing structure, native chitosan showed two peaks at 2θ of 10° and 20° (Fig. 3a), however LMWCts gave only one broader peak at 2θ of 20° (Fig. 3b) implying a decrease in crystallinity.

By comparison with high molecular weight chitosan, LMWCts and/or chitosan oligomer possessed not only the solubility at a wide range of pH including neutral one, reduced viscosity, and ease of handling, but also low toxicity (Kean et al., 2005) and fast biodegradability. In addition, chemical and physical modifications of LMWCts might be achieved under mild conditions.

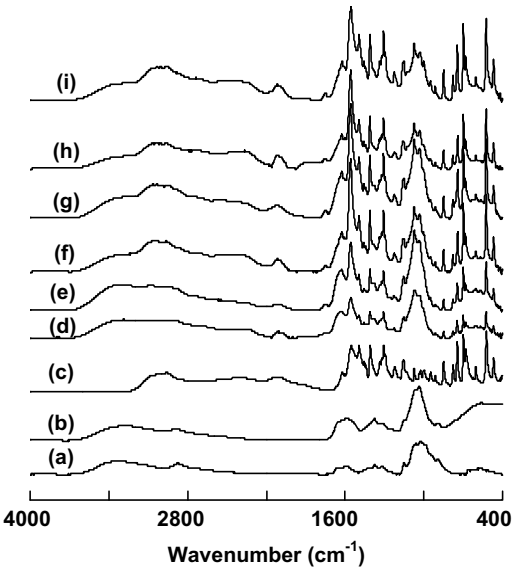

Fig. 1. FT-IR spectra of (a) chitosan, (b) LMWCts, (c) L-phenylalanine, (d) LMWCts-*g*-Phe0.5, (e) LMWCts-*g*-Phe1, (f) LMWCts-*g*-Phe2A, (g) LMWCts-*g*-Phe2B, (h) LMWCts-*g*-Phe3, and (i) LMWCts-*g*-Phe5.

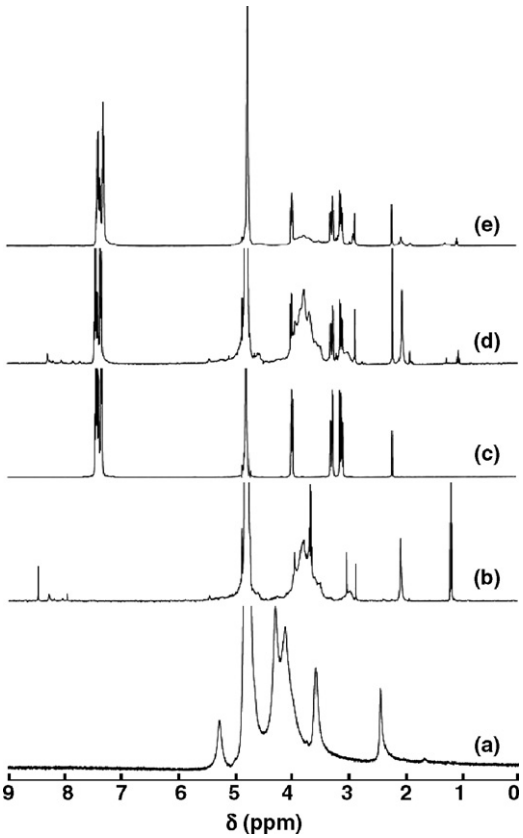

Fig. 2. ^{1}H NMR patterns of (a) chitosan, (b) LMWCts, (c) L-phenylalanine, (d) LMWCts-*g*-Phe0.5, and (e) LMWCts-*g*-Phe5.

3.2. Preparation and characterization of LMWCts-g-Phe

The grafting reaction of Phe onto LMWCts was carried out under simple conditions, i.e., water-based system and room temperature, using carbodiimide (EDC) as a coupling agent and HOBt as a catalyst. The product showed new peaks at 2936 (C–H stretching),

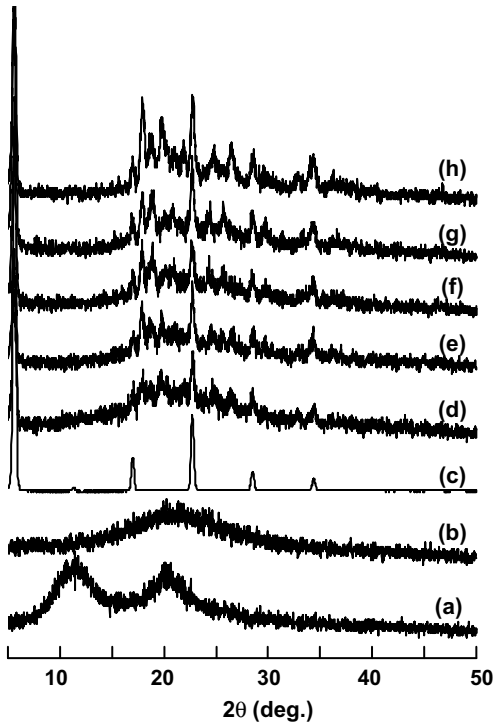

Fig. 3. XRD patterns of (a) chitosan, (b) LMWCts, (c) L-phenylalanine, (d) LMWCts-*g*-Phe0.5, (e) LMWCts-*g*-Phe1, (f) LMWCts-*g*-Phe2A, (g) LMWCts-*g*-Phe3, and (h) LMWCts-*g*-Phe5.

1730 (ester bond), and 700 and 525 cm^{-1} (aromatic ring) (Fig. 1d–i) as well as proton peaks at δ 3.05–3.35 ($C\underline{H}_2$), 4.0 ($C\underline{H}$), and 7.3–7.5 ppm ($C_6\underline{H}_5$) (Fig. 2d–e). The grafting of Phe onto LMWCts occurred randomly at both hydroxyl and amino groups as confirmed from a new ester peak (1730 cm^{-1}) and a higher intensity of amide peaks (1640 and 1557 cm^{-1}), respectively. XRD results also supported the accomplishment of the reaction as illustrated from the peak combination of LMWCts (Fig. 3b) and Phe (Fig. 3c) in the patterns of the products (Fig. 3d–h). It was speculated that the peaks at 2θ of 17°, 23°, 29°, and 34° belonged to Phe, while the other peaks might represent the packing structure induced from a pi–pi stacking or aromatic–aromatic interaction of Phe on the LMWCts-*g*-Phe. The intensity of all peaks increased when the amount of Phe in feed increased suggesting an increase in the extent of Phe grafting on the LMWCts.

The number of Phe units per a grafting chain, so called the degree of polymerization (DP), and the number of grafting chains per 100 glucopyranose rings, so called the degree of substitution (DS) were quantitatively determined by ^{1}H NMR and tabulated in Table 1. When the amount of Phe in feed increases, the DP also increases, e.g., DPs are 2 and 19 when Phe in feed are 0.5 and 5 mol equiv. to pyranose ring, respectively. In other words, the higher the amount of Phe in feed, the longer the grafting chain length. It should be noted that LMWCts consisted of 26 pyranose units, the DP, thus, should not exceed such a value; as a result the maximum amount of Phe in feed used in the present work was limited at 5 mol equiv. to pyranose ring. The DS is hardly altered by varying the amount of Phe in feed, e.g., when the amount of Phe in feed is 0.5–3 mol equiv. to pyranose ring, the DS is in the range of 21–23 corresponding to ~6 grafting chains (Table 1). The DS slightly decreases to 18 (~5 grafting chains), when Phe in feed is 5 mol equiv. to pyranose ring (Table 1). The difficulty to control DS and DP might result from simultaneous grafting and self-linking reactions. However, the increase in % grafting, when the amount of Phe in feed increases, is resulted from the increase in DP (Table 1). One should note that the amount of coupling agent and catalyst hardly affected DP and DS. In addition, the increase in % grafting of Phe was also confirmed from EA technique based on C/N ratio (Table 1). The difference in % grafting determined by ^{1}H NMR and EA techniques might come from the incomplete combustion of samples.

Table 1
Degree of polymerization (DP), degree of substitution (DS), and grafting percentage of L-phenylalanine on LMWCts-*g*-Phe

Samples	DP[a]	DS[b]	% Grafting	
			^{1}H NMR[c]	EA
LMWCts-*g*-Phe0.5	2.22	21.64	48.04	47.86
LMWCts-*g*-Phe1	5.94	20.61	122.42	93.55
LMWCts-*g*-Phe2A	6.60	22.66	149.56	181.63
LMWCts-*g*-Phe2B	6.60	21.68	143.09	174.11
LMWCts-*g*-Phe3	10.40	21.91	227.86	257.93
LMWCts-*g*-Phe5	19.11	17.84	340.92	420.60

[a] DP: Degree of polymerization refers to number of Phe units per a grafting chain determined by ^{1}H NMR; DP = ($I_{\text{aromatic protons}}/5$)/($I_{\text{CH3(acetamide)}}/3$).
[b] DS: Degree of substitution refers to number of grafting chains per 100 glucopyranose rings determined by ^{1}H NMR; DS = [($I_{\text{aromatic protons}}/(5 \times \text{DP})$)/($I_{\text{H3-6(pyranose ring)}}/5$)] × 100.
[c] % Grafting = DP × DS.

The morphology of samples was observed by SEM. In general, chitosan shows flake-like appearance (Fig. 4a), while LMWCts is nanosphere with an average size of ~100 nm (Fig. 4b). After grafting with Phe, the appearance of product depended on the amount of Phe. For example, when % grafting was less than 123, the LMWCts-*g*-Phe performed spherical shape with an average size of ~80 nm (Fig. 4c–d), but when % grafting increased, the particles appeared to combine each other (Fig. 4e). This might be resulted from a pi–pi stacking interaction.

3.3. Complex formation of LMWCts-g-Phe and DNA

Due to the nano-size and environmentally friendly characteristic (biodegradability), the LMWCts-*g*-Phe is expected to be suitable for pharmaceutical and biomedical applications, especially as a carrier for delivery of bioactive molecules, such as drugs, proteins, vaccines, genes, and DNA to the target organs. In the present work, DNA was chosen as a model molecule.

The complexes of LMWCts-*g*-Phe and DNA (LMWCts-*g*-Phe/DNA) were prepared by a complex coacervation method in an aqueous solution, without the addition of acid, which preserved biological activities of DNA. In general, pK_a of native chitosan is ~6.0–6.5 (Schatz, Pichot, Delair, Viton, & Domard, 2003); however, the ones belonging to the LMWCts and LMWCts-*g*-Phe might be higher as confirmed from the solubility in a wide range of pH. Soon after dropping LMWCts-*g*-Phe/water solution into DNA/50 mM aqueous Na_2SO_4 solution with an equi-volume at 50 °C during vortex at the highest speed, the solution turned turbid implying the complex formation. It was speculated that the complex was formed via electrostatic interaction between the cationic LMWCts-*g*-Phe (NH_3^+) and the anionic DNA molecules (PO_4^{3-}).

3.3.1. Morphology of LMWCts-g-Phe/DNA complexes

The individual complexes performed various shapes with an average size of ~50–150 nm as observed by SEM (Fig. 4f–g) and ~40–70 nm by TEM (Fig. 5). The different shapes of the chitosan/DNA complexes were also investigated by Koping-Hoggard et al. (2004). Moreover, SEM micrograph revealed that some particles formed aggregates with an approximate size of ~300–500 nm and those aggregates showed agglomeration (Fig. 4h). The shape and size of the complexes prepared from LMWCts-*g*-Phe0.5 and LMWCts-*g*-Phe1 did not significantly differ from the one from

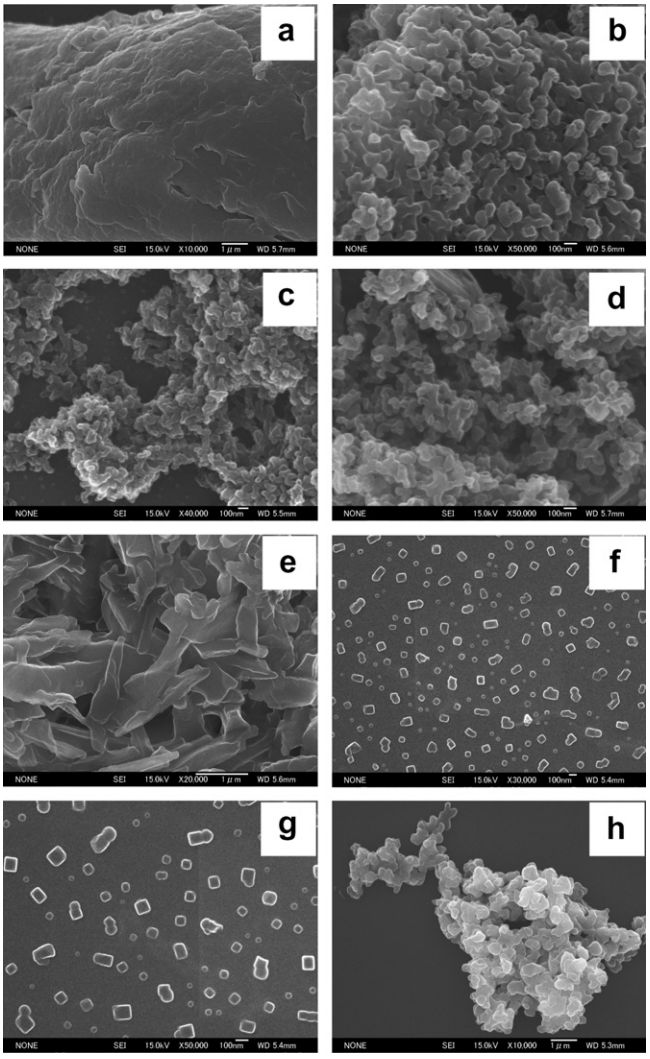

Fig. 4. SEM micrographs of (a) chitosan (10,000×), (b) LMWCts (50,000×), (c) LMWCts-*g*-Phe0.5 (40,000×), (d) LMWCts-*g*-Phe1 (50,000×), (e) LMWCts-*g*-Phe5 (20,000×), (f) LMWCts-*g*-Phe1/DNA (30,000×), (g) LMWCts-*g*-Phe1/DNA (50,000×), and (h) LMWCts-*g*-Phe1/DNA (10,000×).

LMWCts implying that % grafting of Phe at this level (<123%) did not affect the morphology of the complexes.

3.3.2. Surface charge of LMWCts-g-Phe/DNA complexes

To study the effect of sample (1, 2, 3, 4, and 5 mg/mL) and DNA concentrations (0.01, 0.05, and 0.1 mg/mL) on the surface charge of the complex, the zeta potential was measured in a 25 mM aqueous Na_2SO_4 solution at 20 °C. Fig. 6 shows that the zeta potential increased as the concentration of sample, LMWCts and LMWCts-*g*-Phe, increased, e.g., the zeta potentials were ∼−8 and +1 mV when the concentrations of sample were 1 and 5 mg/mL, respectively for 0.01 mg/mL of DNA solution (Fig. 6a). On the contrary, the zeta potential decreased as DNA concentration increased, e.g., the zeta potentials were ∼−8 and −12 mV when the concentrations of DNA were 0.01 (Fig. 6a) and 0.1 mg/mL (Fig. 6c), respectively for 1 mg/mL of sample solution. The zeta potential reached zero (neutral surface) when the concentrations of sample were 2, 3, and 5 mg/mL for DNA concentrations of 0.01, 0.05, and 0.1 mg/mL, respectively. The results implied that the surface charge of the complex depended on the concentrations of sample and DNA used in the complex preparation step.

The zeta potential increased only slightly with a high concentration sample, especially in the case of low DNA concentration, e.g., when the concentration of a sample was about 3–5 mg/mL, the zeta potential increased slightly from ∼0 to +2 mV for 0.01 mg/mL of DNA solution (Fig. 6a). The zeta potentials for LMWCts-*g*-Phe/DNA were not markedly different from those for LMWCts/DNA in all of the sample and DNA concentrations which

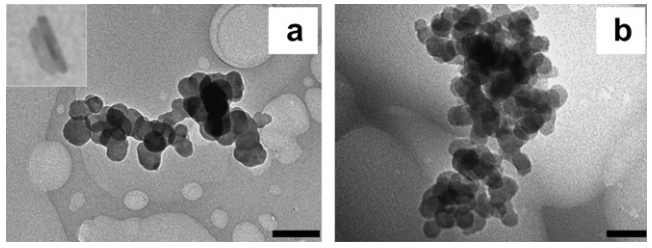

Fig. 5. TEM micrographs of LMWCts-*g*-Phe0.5/DNA; (a) bar = 100 nm and (b) bar = 50 nm.

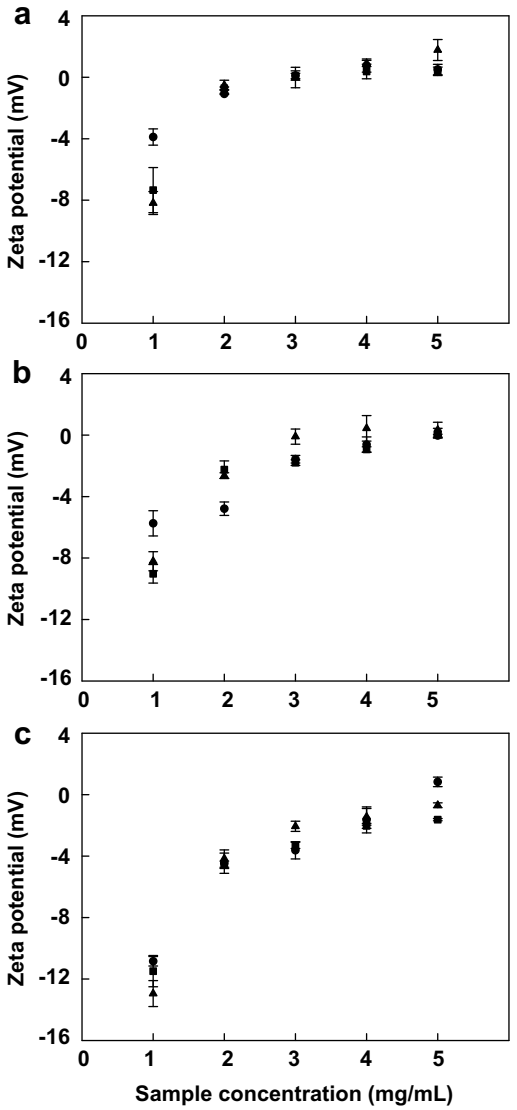

Fig. 6. Zeta potential at 20 °C in 25 mM aqueous Na_2SO_4 of complexes prepared from LMWCts (●), LMWCts-*g*-Phe0.5 (■), and LMWCts-*g*-Phe1 (▲) at various concentrations; when DNA concentrations are (a) 0.01 mg/mL, (b) 0.05 mg/mL, and (c) 0.1 mg/mL. The data are expressed as mean values ± standard deviation (n = 3).

ranged from −12 to +2 mV for the present experimental conditions.

The surface charge should be considered when the complex is introduced into the body; for example, a highly positive charge (high zeta potential) should be avoided because it might cause toxic side effects for cells, nonspecific interactions between complex and cells, and also exchange reactions of DNA with negatively charged macromolecules existing in the body during delivery (Kircheis and Wagner, 2000; Schatzlein, 2001). Here, 1 mg/mL of sample solution and 0.1 mg/mL of DNA solution were chosen to prepare the complexes for the *in vitro* cytotoxicity test (see Section 3.4) and DNA release study (see Section 3.5). The zeta potentials of the obtained complexes ranged from −10 to −14 mV (Fig. 6c) implying that the complex surface was negatively charged and mainly covered with DNA.

3.3.3. Evaluation of DNA loading efficiency

The loading efficiency of DNA into the complex was calculated based on the total amount of DNA added in the complex preparation step. The % DNA loading efficiency decreased as the sample concentration increased, e.g., % DNA loading efficiency was ~80–90 for the complex prepared from 1 mg/mL of sample solution, and ~40–60 for the one from 5 mg/mL in the case of LMWCts-*g*-Phe (data not shown). However, LMWCts gave a higher % DNA loading efficiency than did LMWCts-*g*-Phe for all of the tested sample concentrations. This may have resulted from an electrostatic interaction between the large number of free amino groups on the LMWCts and the negatively charged DNA.

3.4. In vitro cytotoxicity test

The cytotoxicity of materials is one of the most important sources of information to tell us whether those materials are suitable for pharmaceutical and biomedical uses. Here, fibroblasts were applied as model cells. The morphology and viability of cells were observed after incubating the cells in a sample/DMEM culture medium solution for 22 h at 37 °C in a humidified 5% CO_2/95% air atmosphere. It was found that for all samples the appearances of incubated cells were normal and without significant changes in cell morphology (data not shown).

The % viability of cells was evaluated by WST-1 method (Berridge et al., 1996). This method is based on the ability of mitochondrial dehydrogenases in viable cells to convert WST-1 into WST-formazan, which can be quantitatively detected by spectrophotometer at λ_{max} of 450 nm. The obtained value is, thus, related to the number of viable cells. LMWCts and LMWCts-*g*-Phe gave the % cell viability in the range of 76–105 indicating a very low cytotoxicity to fibroblasts (Fig. 7A-C). Generally, DNA is a non-toxic material with ~99–119 %viability at present (Fig. 7D). For the complexes, the % cell viability was about 76–111 implying a less toxicity of LMWCts/DNA and LMWCts-*g*-Phe/DNA (Fig. 7E-G). However, the LMWCts/DNA at the concentration of 0.5 mg/mL gave 37% cell viability. It was speculated that the complex at high concentration might act as a surfactant to remove the adhered cells and/or impede the cell adhesion resulting in a decreased viable cell number. This data suggested that the threshold concentration of the LMWCts/DNA is limited at 0.4 mg/mL. One should notice that LMWCts-*g*-Phe/DNA possesses lower cytotoxicity than LMWCts-*g*-Phe, except at high concentration (0.5 mg/mL) in which the removal of adhered cells and/or the impediment of cell adhesion might be involved. In a similar way, LMWCts/DNA at low concentration (0.1–0.2 mg/mL) shows higher % cell viability than LMWCts, and vice versa at high concentration (0.3–0.5 mg/mL). Overall, the cytotoxicity of LMWCts-*g*-Phe and its complexes were comparable to that of LMWCts and its complexes when the sample concentration was less than 0.4 mg/mL.

3.5. Study on in vitro DNA release

The releasing profiles of DNA from the LMWCts/DNA and LMWCts-*g*-Phe/DNA complexes were investigated *in vitro* at 37 ± 0.5 °C for 44 days in various buffers, i.e., citric acid/trisodium citrate buffer (pH 3.0), phosphate buffer saline (PBS, pH 7.4), tris buffer (pH 8.0), and carbonate buffer (pH 9.5). Those pHs were models for gut. The physical appearances of all complexes incubated in high pH media, i.e., carbonate and tris buffers were observed by the naked eye to have swelled and completely disappeared within between 2 and 4 days. In contrast, the complexes shrank and became darker in the low pH medium, i.e., citric acid/trisodium citrate buffer. For PBS, although the complexes swelled and gradually disappeared, a residual existed during the experimental period. It should be noted that the swelling and the disappearance of the LMWCts-*g*-Phe/DNA were more significant than those of the LMWCts/DNA incubated in all buffers. This might be explained by the ease of dissolution and/or degradation of the LMWCts-*g*-Phe owing to the bulky phenylalanine side chains. The faster disappearance of LMWCts-*g*-Phe1/DNA than LMWCts-*g*-Phe0.5/DNA also supported our explanation.

The amount of released DNA was measured by a spectrophotometer at 258 nm. It should be pointed out that the LMWCts/DNA and LMWCts-*g*-Phe/DNA incubated in all media gave similar releasing profiles (Fig. 8). The release of DNA was markedly divided into two stages based on the release rate (the slope of DNA releasing profiles). For the initial stage, i.e., the first 24 h for carbonate and tris buffers and 333 h for citric acid/trisodium citrate buffer and PBS, the release rate is very fast (burst effect), especially in the cases of high pH media, i.e., carbonate and tris buffers (Fig. 8). The mechanism of DNA release in this stage might be explained by the diffusion of DNA localized at the complex surface, which might be involved with the concentration gradient. The diffusion of DNA was enhanced at

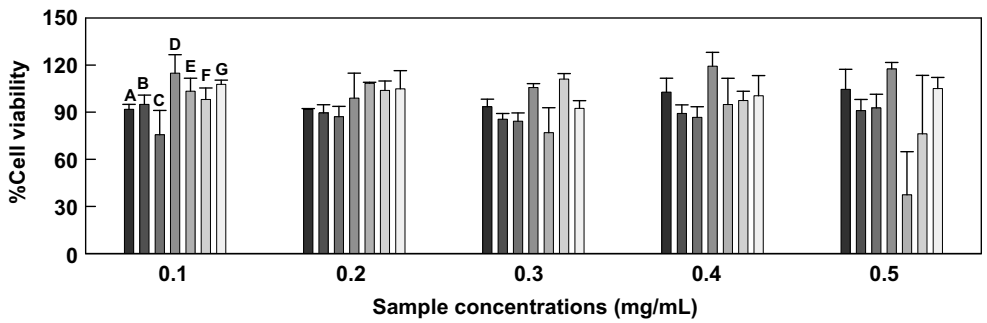

Fig. 7. %Cell viability at various concentrations of A: LMWCts, B: LMWCts-*g*-Phe0.5, C: LMWCts-*g*-Phe1, D: DNA, E: LMWCts/DNA, F: LMWCts-*g*-Phe0.5/DNA, and G: LMWCts-*g*-Phe1/DNA. The data are expressed as mean values ± standard deviation (n = 3–4).

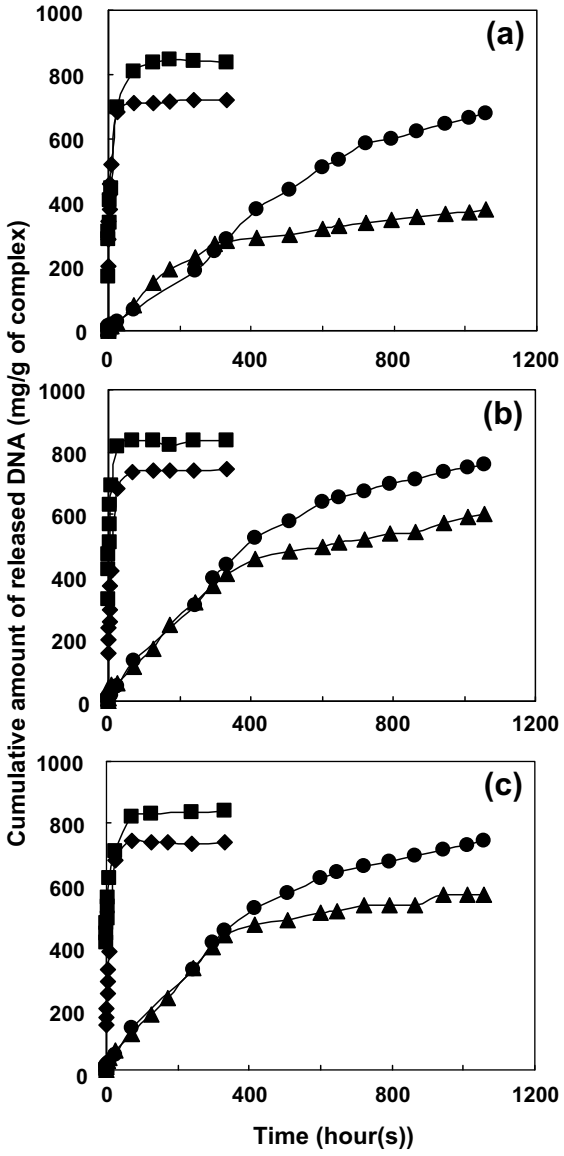

Fig. 8. *In vitro* releasing profiles of DNA at 37 ± 0.5 °C from (a) LMWCts/DNA, (b) LMWCts-*g*-Phe0.5/DNA, and (c) LMWCts-*g*-Phe1/DNA in various buffers; carbonate buffer (pH 9.5, ♦), tris buffer (pH 8.0, ■), phosphate buffer saline (PBS, pH 7.4, ▲), and citric acid/trisodium citrate buffer (pH 3.0, ●).

high pH due to the deprotonation of cationic material (LMWCts or LMWCts-*g*-Phe); as a result the electrostatic or ionic interaction between the material and DNA was null and DNA was eventually discharged very fast. On the contrary, the electrostatic interaction between the cationic material and DNA was strong in the low pH medium (pH < pK_a), i.e., citric acid/trisodium citrate buffer. In the case of PBS, since pK_a of LMWCts and LMWCts-*g*-Phe is higher than that of native chitosan (~6.0–6.5 (Schatz et al., 2003)), the deprotonation of the LMWCts and LMWCts-*g*-Phe in PBS was, thus, relatively low compared to that in carbonate and tris buffers resulting in the slower initial DNA release rate. The first-day release percentages of DNA from the complexes incubated in carbonate, tris, PBS, and citric acid/trisodium citrate buffers (calculation based on the maximum released DNA in each buffer) were 92, 84, 12, and 7, respectively, implying that DNA was more controllably released in neutral and low pH media than in high pH ones.

For the second stage, the release rate is relatively slow, especially in the cases of carbonate and tris buffers (Fig. 8). This might be due to the small amount of DNA left inside and/or at the surface of the complexes. The small release of DNA during this stage might mainly occur via the degradation of cationic material. The release of DNA in carbonate and tris buffers reached the plateau within 69 h, while to reach a plateau in PBS and citric acid/trisodium citrate buffer required longer time (>44 days). In other words, the release of DNA from the LMWCts/DNA and LMWCts-*g*-Phe/DNA finished within 3 days in carbonate and tris buffers, while more than 44 days in PBS and citric acid buffers. This might be caused by the stronger electrostatic interaction between the cationic material and DNA resulting in the longer release period.

By considering the release in high pH media, the amount of released DNA in tris buffer was higher than that in carbonate one (Fig. 8). We speculated that carbonate buffer at pH 9.5 was too severe for DNA to stay in its native form. For the release in neutral and low pH media, it was expected that the amount of released DNA in citric acid/trisodium citrate buffer should be lower than that in PBS, but the result was contrary, especially after 333 and 241 h for the LMWCts/DNA and LMWCts-*g*-Phe/DNA, respectively (Fig. 8). This might be resulted from the difference in dissolution and/or degradation rate of cationic material after 10- to 14-day incubation.

LMWCts-*g*-Phe/DNA gave a higher amount of released DNA than LMWCts/DNA in PBS (Fig. 9a) and citric acid/trisodium citrate buffer (Fig. 9b). This might be due to the loosened structure of LMWCts-*g*-Phe and the destruction of inter- and intramolecular hydrogen bonds caused by the introduction of bulky phenylalanine chains; as a result, the swelling as well as the degradation and/or dissolution of the LMWCts-*g*-Phe/DNA were higher than those of the LMWCts/DNA, and a higher amount of DNA was consequently released. The other point might concern the weak electrostatic interaction between LMWCts-*g*-Phe and DNA resulted from small amount of free amino groups. For the release of DNA in high pH media, it was speculated that such processes took place rapidly so that the difference in the amount of released DNA from the LMWCts-*g*-Phe/DNA and LMWCts/DNA was not significant.

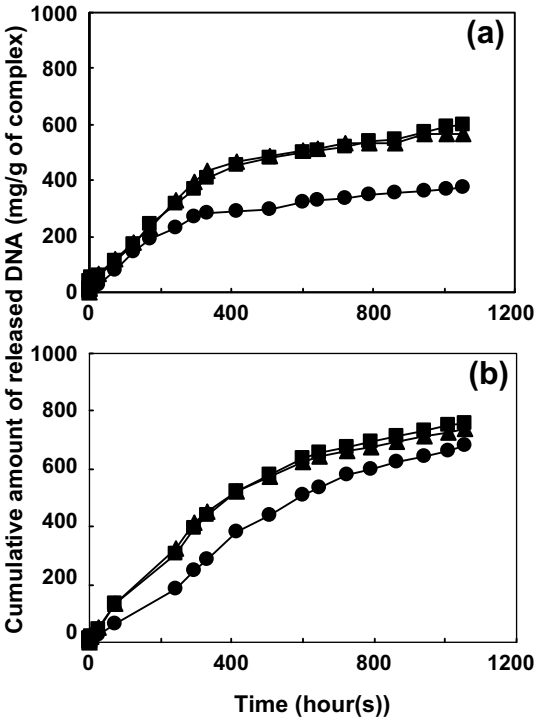

Fig. 9. *In vitro* releasing profiles of DNA at 37 ± 0.5 °C from LMWCts/DNA (●), LMWCts-*g*-Phe0.5/DNA (■), and LMWCts-*g*-Phe1/DNA (▲) in various buffers; (a) phosphate buffer saline (PBS, pH 7.4) and (b) citric acid/trisodium citrate buffer (pH 3.0).

4. Conclusions

Low molecular weight chitosan grafted with L-phenylalanine (LMWCts-*g*-Phe) was synthesized by a carbodiimide coupling reaction under mild condition. The obtained LMWCts-*g*-Phe consisted of 26 pyranose units with 5–6 grafting chains; each grafting chain was composed of 2–19 U of Phe when the amount of Phe in feed was varied in the range of 0.5–5 mol equiv. to pyranose ring. SEM micrographs revealed that the LMWCts-*g*-Phe with short grafting chain (DP < 6) was spherical particle with an average size of ~80 nm. The present work also reported one of the feasible applications of the LMWCts-*g*-Phe, i.e., as a carrier for negatively charged molecules. DNA was chosen as a model molecule. The complexes of LMWCts-*g*-Phe and DNA (LMWCts-*g*-Phe/DNA) performed various shapes with an average size of ~50–150 nm as observed by SEM and ~40–70 nm by TEM. The LMWCts-*g*-Phe/DNA possessed a high % DNA loading efficiency (~80–90), negatively charged surface (~−11 to −14 mV of zeta potential), and very low toxicity to fibroblasts (~76–111 %cell viability). The release of DNA from the complexes incubated at 37 ± 0.5 °C in carbonate (pH 9.5) and tris buffers (pH 8.0) finished within 3 days, while the ones in PBS (pH 7.4) and citric acid/trisodium citrate buffer (pH 3.0) gave much more sustained release, i.e., more than 44 days. By comparing to the LMWCts, even the LMWCts-*g*-Phe gave lower % DNA loading efficiency; the amount of released DNA was higher over the experimental period, especially in PBS and citric acid/trisodium citrate buffer. The less cytotoxicity of the LMWCts-*g*-Phe and its complexes (LMWCts-*g*-Phe/DNA) was comparable to that of the LMWCts and its complex (LMWCts/DNA). In addition, the LMWCts-*g*-Phe/DNA incubated in all tested buffers showed a higher degree of swelling and faster degradability than LMWCts/DNA. These results promote that the LMWCts-*g*-Phe could be one of the promising carriers for negatively charged bioactive molecules.

Acknowledgements

This work was financially supported by the Japan Society for the Promotion of Science (JSPS), Japan (P05133). One of the authors (R.Y.) thanks Assist. Prof. Michiya Matsusaki (Osaka University, Japan) for the technique and discussion on cell culture.

Appendix A. Supplementary data

Supplementary data associated with this article can be found, in the online version, at doi:10.1016/j.carbpol.2008.07.001.

References

Batista, M. K. S., Pinto, L. F., Gomes, C. A. R., & Gomes, P. (2006). Novel highly-soluble peptide-chitosan polymers: Chemical synthesis and spectral characterization. *Carbohydrate Polymers, 64*, 299–305.

Beena, M. S., Thomas, C., & Sharma, C. P. (1994). Phenylalanine, tryptophan immobilized chitosan beads as adsorbents for selective removal of immunoproteins. *Journal of Biomaterials Applications, 8*(4), 385–403.

Berridge, M. V., Tan, A. S., McCoy, K. D., & Wang, R. (1996). The biochemical and cellular basis of cell proliferation assays that use tetrazolium salts. *Biochemica, 4*, 14–19.

Bozkir, A., & Saka, O. M. (2004). Chitosan nanoparticles for plasmid DNA delivery: Effect of chitosan molecular structure on formulation and release characteristics. *Drug Delivery, 11*, 107–112.

Chi, P., Wang, J., & Liu, CS. (2008). Synthesis and characterization of polycationic chitosan-graft-poly(L-lysine). *Materials Letters, 62*(1), 147–150.

Choi, Y. H., Lui, F., Kim, J. S., Choi, Y. K., Park, J. S., & Kim, S. W. (1998). Polyethylene glycol-grafted poly-L-lysine as polymeric gene carrier. *Journal of Controlled Release, 54*(1), 39–48.

Chung, T. W., Lu, Y. F., Wang, S. S., Lin, Y. S., & Chu, S. H. (2002). Growth of human endothelial cells on photochemically grafted Gly-Arg-Gly-Asp (GRGD) chitosans. *Biomaterials, 23*, 4803–4809.

Chung, T. W., Lu, Y. F., Wang, H. Y., Chen, W. P., Wang, S. S., Lin, Y. S., et al. (2003). Growth of human endothelial cells on different concentrations of Gly-Arg-Gly-Asp grafted chitosan surface. *Artificial Organs, 27*(2), 155–161.

Godbey, W. T., Wu, K. K., & Mikos, A. G. (2001). Poly(ethylenimine)-mediated gene delivery affects endothelial cell function and viability. *Biomaterials, 22*, 471–480.

Gomes, P., Gomes, C. A. R., Batista, M. K. S., Pinto, L. F., & Silva, P. A. P. (2008). Synthesis, structural characterization and properties of water-soluble *N*-(gamma-propanoyl-amino acid)-chitosans. *Carbohydrate Polymers, 71*(1), 54–65.

Ho, M. H., Wang, D. M., Hsieh, H. J., Lui, H. C., Hsien, T. Y., Lai, J. Y., et al. (2005). Preparation and characterization of RGD-immobilized chitosan scaffolds. *Biomaterials, 26*, 3197–3206.

Hu, F. Q., Zhao, M. D., Yuan, H., You, J., Du, Y. Z., & Zeng, S. (2006). A novel chitosan oligosaccharide-steric acid micelles for gene delivery: Properties and in vitro transfection studies. *International Journal of Pharmaceutics, 315*, 158–166.

Ishii, H., Minegishi, M., Lavitpichayawong, B., & Mitani, T. (1995). Synthesis of chitosan-amino acid conjugates and their use in heavy metal uptake. *International Journal of Biological Macromolecules, 17*(1), 21–23.

Karakecili, A. G., & Gumusderelioglu, M. (2008). Physico-chemical and thermodynamic aspects of fibroblastic attachment on RGDS-modified chitosan membranes. *Colloids and Surfaces, B Biointerfaces, 61*(2), 216–223.

Kean, T., Roth, S., & Thanou, M. (2005). Trimethylated chitosans as non-viral gene delivery vectors: Cytotoxicity and transfection efficiency. *Journal of Controlled Release, 103*, 643–653.

Kiang, T., Wen, J., Lim, H. W., & Leong, K. W. (2004). The effect of the degree of chitosan deacetylation of the efficiency of gene transfection. *Biomaterials, 25*(22), 5293–5301.

Kirsebom, H., Aguilar, M. R., Roman, J. S., Fernandez, M., Prieto, M. A., & Bondar, B. (2007). Macroporous scaffolds based on chitosan and bioactive molecules. *Journal of Bioactive and Compatible Polymers, 22*(6), 621–636.

Koping-Hoggard, M., Mel' nicova, Y. S., Varum, K. M., Lindman, B., & Artursson, P. (2003). Relationship between the physical shape and the efficiency of oligomeric chitosan as a gene delivery system in vitro and in vivo. *The Journal of Gene Medicine, 5*, 130–141.

Koping-Hoggard, M., Varum, K. M., Issa, M., Danielsen, S., Christensen, B. E., Stokke, B. T., et al. (2004). Improved chitosan-mediated gene delivery based on easily dissociated chitosan polyplexes of highly defined chitosan oligomers. *Gene Therapy, 11*, 1441–1452.

Kurita, K., Hayakawa, M., Nishiyama, Y., & Harata, M. (2002). Polymeric asymmetric reducing agents: preparation and reducing performance of chitosan/dihydronicotinamide conjugates having L- and D-phenylalanine spacer arms. *Carbohydrate Polymers, 47*, 7–14.

Lee, M., Nah, J. W., Kwon, Y., Koh, J. J., Ko, K. S., & Kim, S. W. (2001). Water-soluble and low molecular weight chitosan-based plasmid DNA delivery. *Pharmaceutical Research, 18*(4), 427–431.

Lee, K. Y. (2005). Stability of ionic complexes prepared from plasmid DNA and self-aggregated chitosan nanoparticles. *Macromolecular Research, 13*(6), 542–544.

Li, J., Yang, C., Li, H., Wang, X., Goh, S. H., Ding, J. L., et al. (2006). Cationic supramolecules composed of multiple oligoethylenimine-grafted β-cyclodextrins threaded on a polymer chain for efficient gene delivery. *Advanced Materials, 18*, 2969–2974.

Mao, H. Q., Roy, K., Troung-Le, V. L., Janes, K. A., Lin, K. Y., Wang, Y., et al. (2001). Chitosan-DNA nanoparticles as gene carriers: synthesis, characterization and transfection efficiency. *Journal of Controlled Release, 70*(3), 399–421.

Muzzarelli, R. A. A., Tanfani, F., Emanuelli, M., & Bolognini, L. (1985). Aspartate glucan, glycine glucan and serine glucan for the collection of cobalt and copper from solutions and brines. *Biotechnology and Bioengineering, 27*(8), 1115–1121.

Peng, J., Xing, X., Wang, K., Tan, W., He, X., & Huang, S. (2005). Influence of anions on the formation and properties of chitosan-DNA nanoparticles. *Journal of Nanoscience and Nanotechnology, 5*, 713–717.

Ravi Kumar, M. N. V., Bakowsky, U., & Lehr, C. M. (2004). Preparation and characterization of cationic PLGA nanospheres as DNA carriers. *Biomaterials, 25*, 1771–1777.

Ravi Kumar, M. N. V., Muzzarelli, R. A. A., Muzzarelli, C., Sashiwa, H., & Domb, A. J. (2004). Chitosan chemistry and pharmaceutical perspectives. *Chemical Reviews, 104*, 6017–6084.

Richardson, S. C. W., Kolbe, H. V. J., & Duncan, R. (1999). Potential of low molecular mass chitosan as a DNA delivery system: Biocompatibility, body distribution and ability to complex and protect DNA. *International Journal of Pharmaceutics, 178*, 231–243.

Schatz, C., Pichot, C., Delair, T., Viton, C., & Domard, A. (2003). Static light scattering studies on chitosan solutions: From macromolecular chains to colloidal dispersions. *Langmuir, 19*(23), 9896–9903.

Schatzlein, A. G. (2001). Non-viral vectors in cancer gene therapy: Principles and progress. *Anti-Cancer Drugs, 12*(4), 275–304.

Segura, T., Volk, M. J., & Shea, L. D. (2003). Substrate-mediated DNA delivery: Role of the cationic polymer structure and extent of modification. *Journal of Controlled Release, 93*, 69–84.

Son, S., Chae, S. Y., Choi, C., Kim, M. Y., Ngugen, V. G., Jang, M. K., et al. (2004). Preparation of a hydrophobized chitosan oligosaccharide for application as an efficient gene carrier. *Macromolecular Research, 12*(6), 573–580.

Tsuguhei, K., & Tatsuaki, Y. Improved method for manufacture of low molecular-weight chitosans and chitooligomers. JP 09031104, 1997-02-04.

Wu, Y., Zheng, Y., Yang, W., Wang, C., Hu, J., & Fu, S. (2005). Synthesis and characterization of a novel amphiphilic chitosan-polylactide graft copolymer. *Carbohydrate Polymers, 59*, 165–171.

Zhu, H., Ji, J., Lin, R., Gao, C., Feng, L., & Shen, J. (2002). Surface engineering of poly(D,L-lactic acid) by entrapment of chitosan-based derivatives for the promotion of chondrogenesis. *Journal of Biomedical Materials Research, 62*(4), 532–539.